

Analysis of Adenosine A_{2a} Receptor Stability: Effects of Ligands and Disulfide Bonds[†]

Michelle A. O'Malley,[‡] Andrea N. Naranjo, Tzvetana Lazarova,[§] and Anne S. Robinson*

Department of Chemical Engineering, University of Delaware, 150 Academy Street, Newark, Delaware 19716, United States

[‡]*Current address: Department of Biology, Massachusetts Institute of Technology, 77 Massachusetts Ave.,*

Cambridge, MA 02139. §Current address: Departament de Bioquímica i Biologia Molecular and Centre d'Estudis en Biofísica, Unitat de Bifísica, Edifici Medicina, Universitat Autònoma de Barcelona, 08193 Bellaterra, Spain.

Received July 21, 2010; Revised Manuscript Received September 17, 2010

ABSTRACT: G protein-coupled receptors (GPCRs) constitute the largest family of integral membrane proteins present in all eukaryotic cells, yet relatively little information about their structure, folding, and stability has been published. In this work, we describe several approaches to characterizing the conformational stability of the human adenosine A_{2a} receptor (hA_{2a}R). Thermal denaturation and chemical denaturation were not reversible, yet clear differences in the unfolding behavior were observed upon ligand binding via circular dichroism and fluorescence spectrometry. We found that the stability of hA_{2a}R was increased upon incubation with the agonist N⁶-cyclohexyladenosine or the antagonist theophylline. When extracellular disulfide bonds were reduced with a chemical reducing agent, the ligand binding activity decreased by ~40%, but reduction of these bonds did not compromise the unfolding transition observed via urea denaturation. Overall, these approaches offer a general strategy for characterizing the effect of surfactant and ligand effects on the stability of GPCRs.

Members of the family of membrane proteins classified as G protein-coupled receptors (GPCRs)¹ are among the most desirable targets for pharmaceutical development because of their predominant role in cellular signaling (1). All GPCRs are integral membrane proteins that are characterized by their seven α -helical transmembrane domains and their ability to initiate intracellular signaling via trimeric G protein activation following ligand binding.

GPCRs play critical roles in several diseases, yet the structural biology of these proteins remains poorly characterized, limiting progress toward the rational design of pharmaceuticals (2). Currently, four high-resolution structures (rhodopsin, β_1 adrenergic, β_2 adrenergic, and adenosine A_{2a} receptors) have been determined from this ~800-member GPCR superfamily, providing some insight into the conserved structural features within this complex protein family (3–6). Although these recently determined structures are significant steps toward an understanding of GPCR structure–function relationships, more information is needed before such data can be readily translated into the design

of effective therapeutics, in part because only the inactive states of the receptors were resolved, with the exception of rhodopsin. In the case of the human adenosine A_{2a} receptor (hA_{2a}R) crystal structure, a C-terminal truncation (Δ 317) and the substitution of T4 lysozyme for intracellular loop 3 were used to facilitate crystallization (4); this variant lacks some key interactions, such as G protein coupling and native agonist preferences, but has been of value in identifying antagonist leads in virtual screening (4, 7, 8). Structural analysis of GPCRs in more dynamic physiological conformations or with a variety of ligands will help address issues pertaining to ligand specificity and reveal critical interactions that underlie receptor function for individual GPCRs.

In our lab, we have readily expressed and purified 6–10 mg/L full-length hA_{2a}R in an active ligand-binding form from a yeast expression system (9–13), facilitating our studies. Using this purified receptor, we have employed several biophysical techniques to elucidate the effects of agonist and antagonist molecules on the stability of hA_{2a}R. Also, with the discovery of an unusually high number of disulfide bonds identified during crystallography (4), we hypothesized that hA_{2a}R stability might be sensitive not only to ligand association but also to the presence of critical extracellular disulfide bonds.

Analysis of this receptor may serve as a basis for more broadly clarifying critical aspects of receptor stability within the GPCR superfamily. In addition, identification of conditions that promote the conformational stability of full-length hA_{2a}R should facilitate crystallography and characterization of active state conformations.

EXPERIMENTAL PROCEDURES

Expression and Purification of hA_{2a}R-His₁₀. A vacuolar protease-deficient strain of *Saccharomyces cerevisiae*, BJ5464

[†]This research was supported by NSF-IGERT (M.A.O. and A.N.N.), a NASA-Harriett G. Jenkins Predoctoral Fellowship (M.A.O.), the National Science Foundation Graduate Research Fellowship Program (A.N.N.), MCI-BF02009-08758/BMC (T.L.), and National Institutes of Health Grant RR15588.

*To whom correspondence should be addressed: 150 Academy St., Newark, DE 19716. Telephone: (302) 831-0557. Fax: (302) 831-1048. E-mail: asr@udel.edu.

¹Abbreviations: CHA, N⁶-cyclohexyladenosine; CPM, 7-(diethylamino)-3-(4'-maleimidylphenyl)-4-methylcoumarin; GPCR, G protein-coupled receptor; hA_{2a}R, human adenosine A_{2a} receptor; TCEP, tris-(2-carboxyethyl)phosphine; DDM, dodecyl β -D-maltoside; CHAPS, 3-(3-cholamidopropyl)dimethylammonio propane sulfonate; CHS, cholesterol hemisuccinate; hA_{2a}R-His₁₀, hA_{2a}R with a C-terminal deca-histidine tag; CD, circular dichroism; CMC, critical micelle concentration; DTT, dithiothreitol, T_{1/2}, mid-point of unfolding.

(MAT α ura3-52 trp1 leu2 Δ 1 his Δ 200 pep::HIS3 prb Δ 1.6R can1 GAL), containing the multi-integrating pITy-hA₂aR-His₁₀ plasmid was used for overexpression and purification of hA₂aR-His₁₀ as described previously (12). Specific radioligand binding is readily detectable for hA₂aR-His₁₀ localized within the yeast plasma membrane prior to solubilization (12, 13) and corresponds to the affinity preferences observed for native hA₂aR (9). After purification and buffer exchange, purified hA₂aR-His₁₀ was reconstituted in mixed micelles consisting of 0.1% dodecyl β -D-maltoside (DDM), 0.1% 3-(3-cholamidopropyl)dimethylammonio propane sulfonate (CHAPS), and 0.02% cholesteryl hemisuccinate (CHS) (Anatrace, Maumee, OH) in 50 mM sodium phosphate buffer (pH 7.0), which has been shown to promote activity of reconstituted hA₂aR in vitro (12).

Prior to biophysical measurements, UV-vis spectra for each protein sample were recorded (230–650 nm) to verify protein content (absorbance at \sim 280 nm) and rule out any potential aggregation of the sample (absorbance at \sim 600 nm). A protein purity of $>95\%$ was also verified through Coomassie staining of sodium dodecyl sulfate–polyacrylamide gel electrophoresis (SDS–PAGE) for all samples. Radioligand binding activity was verified for purified hA₂aR-His₁₀ utilized for biophysical experiments. Each batch of purified, micelle-reconstituted hA₂aR-His₁₀ was used within a 2 week time span, as receptor activity was found to decrease after approximately 20 days when the batch was stored at 4 °C.

Reduction of Disulfide Bonds. Reduction of extracellular disulfide bonds within hA₂aR was achieved via incubation with tris(2-carboxyethyl)phosphine (TCEP) (Thermo-Fisher, Chicago, IL). TCEP was the preferred reducing agent in these studies because of its general compatibility with spectroscopic and biophysical measurements. Surfactant-solubilized hA₂aR-His₁₀ was incubated with 5 mM dithiothreitol (DTT) or various concentrations of TCEP (from 0.5 to 10 mM), separated via electrophoresis via 12% SDS–PAGE, and blotted onto nitrocellulose for Western blot analysis as described previously (12). The mobility of TCEP-treated samples was compared to that of hA₂aR-His₁₀ without TCEP addition. Receptors with one or more reduced disulfide bonds are evident by a shift in mobility compared to that of untreated receptors, as has been previously reported for hA₂aR heterologously expressed in yeast (9).

Ligand Binding. For experiments in which free ligand was added to purified receptors, *N*⁶-cyclohexyladenosine (CHA) (Sigma, St. Louis, MO) and theophylline (Sigma) (14) served as representative agonist and antagonist molecules, respectively. Purified hA₂aR-His₁₀ was typically incubated with 100 μ M CHA or theophylline, well above the affinity constant for competitor (K_i) values of 1.5–4 μ M for CHA (15, 16) and 1.7–22 μ M for theophylline (17, 18), in competition experiments with [³H]CGS-21,680 or [³H]NECA, respectively, for at least 15 min prior to biophysical analysis.

Radioligand binding was performed to assess the activity of hA₂aR-His₁₀ when it was incubated with increasing concentrations of urea. These studies were conducted at room temperature. Protein was purified as detailed above but was not eluted from nickel resin particles. Concentrated solutions of urea (10 M) were prepared in 50 mM phosphate buffer with a 0.1% DDM/0.1% CHAPS/0.02% CHS mixture using ultrapure urea (MP Biomedicals, Cleveland, OH); the pH was adjusted to 7.0, and solutions were filter-sterilized. Urea solutions were prepared and used the same day to prevent the formation of cyanate and ammonium ions resulting from the decomposition of urea over time (19).

Equal amounts of a resin/protein slurry (at a dilution of \sim 1 – 2 μ L of settled resin/mL of solution) were combined with increasing amounts of ultrapure urea at concentrations ranging from 0 to 8 M and incubated on an end-over-end mixer for approximately 5–6 h. After equilibrium had been reached, samples were aliquoted into a 96-well Millipore Multiscreen Filter B 96-well glass fiber plate and combined with 50 nM agonist [³H]CGS-21,680 (Perkin-Elmer, Wellesley, MA). Resin-bound protein was allowed to incubate on a rotating orbital mixer for 1.5–2 h with the radioligand prior to analysis with a MicroBeta Jet (Perkin-Elmer) scintillation counter. Nonspecific radioligand binding was calculated by incubation of radioligand/urea mixtures with empty resin slurry (without protein bound), which was subtracted from all samples. Previous data from our laboratory (J. A. Butz and A. S. Robinson, unpublished observations) showed that using cells or lysate that were not expressing hA₂aR yielded nonspecific binding data similar to those found using a nonradioactive competitor ligand. Samples were run in triplicate, and error bars represent the standard deviation from the average.

Circular Dichroism. Protein secondary structure was characterized by CD spectroscopy measurements conducted on a Jasco J-810 spectropolarimeter with a Peltier temperature controller, as described previously (12). Spectra were measured from 260 to 196 nm, with 1 nm resolution, with at least three integrations obtained for each spectrum. Protein concentrations used in these experiments were typically 0.2 mg/mL per sample. Thermal scans were performed from 5 to 95 °C, in increments of 5 °C with an incubation of 5 min at each temperature interval. Equilibrium times for unfolding experiments were determined empirically for thermal denaturation studies and deemed sufficient when protein spectra no longer changed with time.

Representative data are reported from three or more independent trials, and error bars represent the standard deviation from the average. Appropriate reference spectra were subtracted in all cases, and mean residue ellipticity calculations were corrected for protein dilution incurred through addition of a ligand solution. Mean residue ellipticity (MRE) was calculated according to

$$\text{MRE} = \frac{0.1 \times \text{ellipticity} \times \text{MW}}{\text{concentration} \times l \times \text{aa}} \quad (1)$$

where ellipticity is in millidegrees, MW is the protein molecular weight in grams per mole, concentration is the sample concentration in milligrams per milliliter, *l* is the path length of the cuvette (0.1 cm), and aa is the number of amino acids per monomer. For hA₂aR-His₁₀, aa is 434 and MW was estimated from the primary sequence of the protein to be 47410 g/mol (20). Secondary structure thermal denaturation was fit to a single transition between two states when possible (19).

Fluorescence Spectroscopy. Fluorescence experiments were performed on an ISS-PC-1 (ISS, Champaign, IL) spectrofluorimeter. Measurements were taken with the excitation polarizer set to 90° and the emission polarizer set to 0° to minimize the effects of light scattering on obtained spectra. Protein concentrations were chosen so that the absorbance of the sample at 280 nm was less than or equal to 0.2 (typically 0.1–0.2 mg/mL protein). Ligand addition measurements were performed as detailed above, with ligand present in the reference cuvette, and we corrected for any dilution of protein resulting from the volumetric addition of ligand in the obtained spectra. For intrinsic tryptophan fluorescence measurements, an excitation wavelength of 290 nm was used and fluorescence was measured between 300

and 450 nm. When the full emission spectra were collected (280–440 nm), excitation was set at 265 nm to eliminate the presence of Rayleigh scattering in the emission spectra.

7-(Diethylamino)-3-(4'-maleimidylphenyl)-4-methylcoumarin (CPM) (Invitrogen, Carlsbad, CA) was used as a thiol-reactive fluorescent probe, which has been previously described for membrane proteins (21). In all cases, CPM was protected from light to minimize photobleaching effects. CPM was dissolved in DMSO at a concentration of 4 mg/mL, aliquoted, and stored at -80°C until it was used. Frozen stocks were thawed and diluted 1:40 in 50 mM sodium phosphate with 0.1% DDM/0.1% CHAPS/0.02% CHS buffer, and 30 μL of this dye was added to a 370 μL sample containing purified protein, or protein with ligand. CPM was allowed to react with samples on an end-over-end mixer at 4°C for at least 70–80 min as this incubation time was necessary to achieve full reaction of CPM with accessible free thiols. Samples incubated with CPM were excited at 387 nm, and emission spectra were collected from 400 to 550 nm.

During thermal denaturation experiments, point emission measurements in which CPM fluorescence was measured at an emission wavelength of 463 nm were taken. CPM fluorescence was normalized to the maximal intensity values to improve

readability of the data shown in Figure 4B. However, the normalization did not alter the $T_{1/2}$ values obtained using a model of a single transition between two states and reported in Table 1. Thermal denaturation experiments for both intrinsic tryptophan and CPM fluorescence experiments were performed using a Peltier temperature controller, set to increase the temperature in 5°C increments. The sample chamber was held at each temperature for 5 min prior to fluorescence acquisition. Each trial was conducted in triplicate, and error bars represent the standard deviation from the average after fluorescence intensity normalization. Data for tertiary structure thermal denaturation were fit to a single transition between two states, where possible.

RESULTS

Conformational Changes in hA_2aR -His₁₀ upon Ligand Binding. The secondary structure of purified, detergent-solubilized full-length hA_2aR with a C-terminal decahistidine tag (hA_2aR -His₁₀) was predominantly α -helical as determined via circular dichroism (CD) measurements, as expected from the recently determined crystal structure (4). To evaluate the impact of bound ligands on receptor secondary and tertiary structure as well as overall thermodynamic stability, we performed biophysical experiments in the presence of agonist and antagonist for hA_2aR . Upon incubation with N^6 -cyclohexyladenosine (CHA) (an A_2aR agonist) and theophylline (an A_2aR antagonist), no discernible change was observed in receptor secondary structure (Figure 2A).

hA_2aR contains seven Trp residues (Figure 1), most of which are located within transmembrane domains, one solvent-exposed on the C-terminus of the receptor, and Trp 246 at a critical site in the ligand binding pocket (7) (Figure 1), which suggested that intrinsic tryptophan fluorescence would serve as a good reporter of conformational changes to the tertiary structure in the presence of agonist and antagonist ligands. Native hA_2aR shows an emission maximum at 328 nm, suggesting a relatively nonpolar environment for the Trp residues (Figure 2B). When the theophylline antagonist binds, the emission maximum was identical

Table 1: Midpoints of Thermal Unfolding ($T_{1/2}$, degrees Celsius) Determined for hA_2aR -His₁₀

	wild type	with TCEP	with CHA	with theophylline
CD $T_{1/2}^a$ ($^{\circ}\text{C}$)	58.9 ± 0.4	55.9 ± 0.4	61.1 ± 0.6	58.4 ± 0.4
CPM fluorescence $T_{1/2}$ ($^{\circ}\text{C}$)	41.7 ± 0.2	ND ^b	46.3 ± 0.5	45.6 ± 0.2

^a $T_{1/2}$ is the midpoint of thermal unfolding; values were determined using a model for a single transition between two states. ^bNot determined. Addition of TCEP to CPM samples resulted in high levels of background fluorescence, preventing determination of thermal unfolding with CPM.

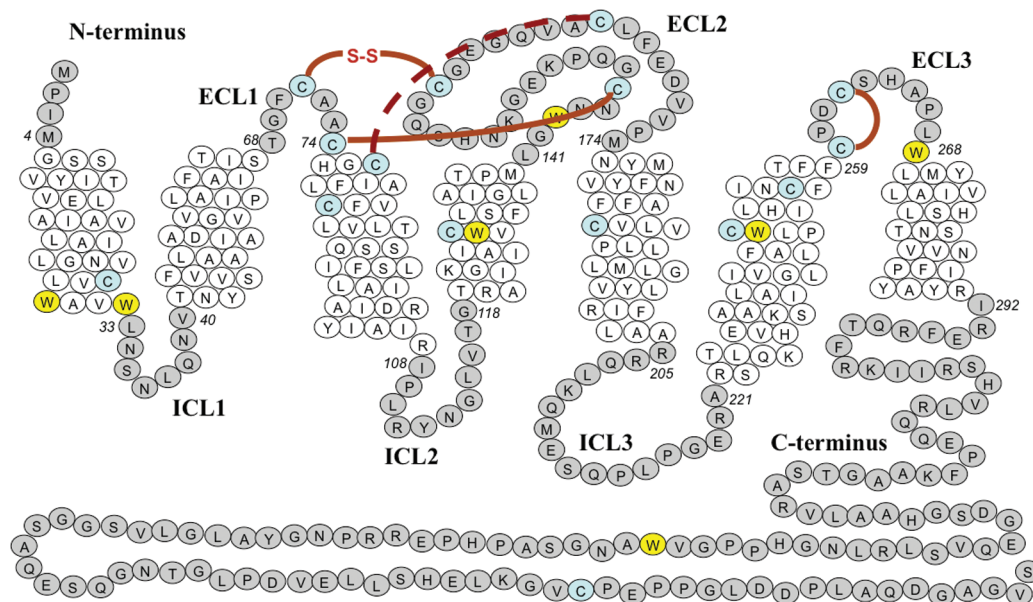


FIGURE 1: Distribution of tryptophan (W) residues and cysteine residues (C) in full-length native hA_2aR . Residues are numbered from the amino terminus and are shown in italics for amino acids that flank the hydrophobic interface. Tryptophan residues are highlighted in yellow, while cysteine residues are highlighted in blue. Intracellular loop regions (ICL) and extracellular loop regions (ECL) are also shown. Disulfide bonds are indicated between paired cysteines. The disulfide bond generally conserved among members of the GPCR superfamily is shown as a red dashed line, while other bonds are displayed as solid red lines.

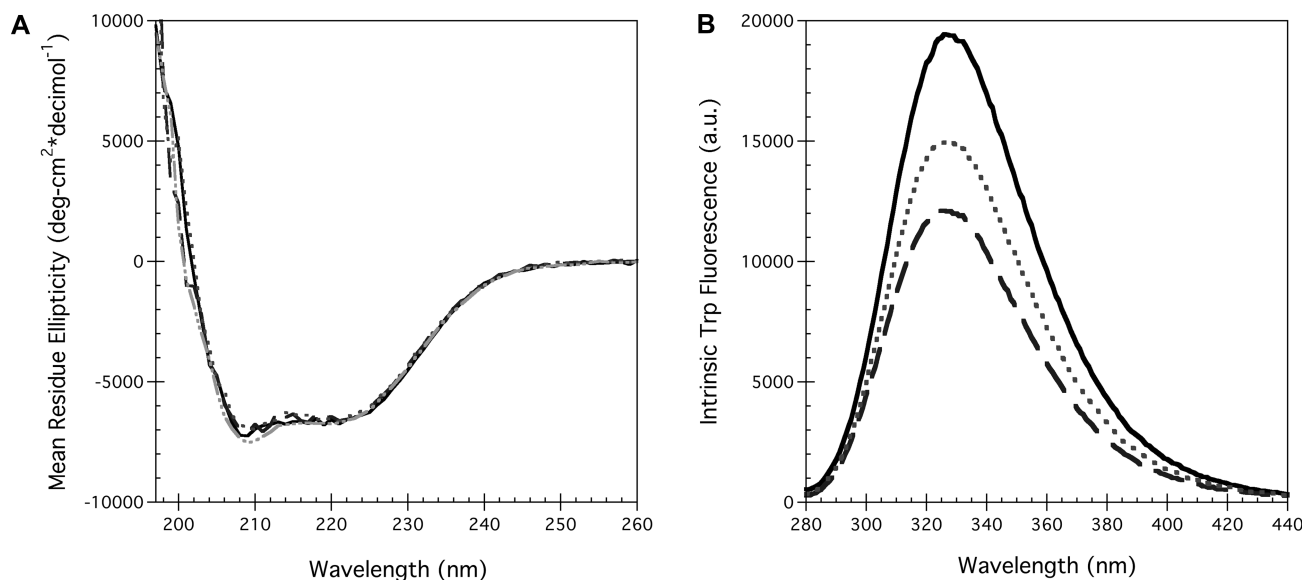


FIGURE 2: Impact of ligand binding and TCEP addition on hA_{2a}R-His₁₀ protein conformation observed via CD (A) and via intrinsic protein fluorescence (excitation wavelength, 265 nm) (B). Unliganded receptors (black), receptors with either CHA agonist (dark gray dashed) or theophylline antagonist (medium gray dotted) at 100 μ M, or receptors reduced with 1 mM TCEP (light gray dashed and dotted). Lines are the interpolated spectra for measurements taken every 1 nm and averaged for three independent data sets.

to that of hA_{2a}R in the absence of ligand but was blue-shifted to approximately 326 nm in the presence of the CHA agonist (Figure 2B). Both ligands showed some absorption at 280 nm, due to the presence of aromatic rings. However, the inner filter effects contributing to the observed decrease in intensity are likely minimal, as shifting the excitation wavelength to minimize ligand absorption yielded similar behavior.

Impact of Disulfide Bonds on hA_{2a}R-His₁₀ Conformation. The crystal structure for a C-terminal truncation of hA_{2a}R fused to T4 lysozyme revealed an extensive disulfide bond network within the extracellular loop regions of the receptor (4). C71–C159, C74–C146, and C77–C166 disulfide bonds tether extracellular loops 1 and 2, while a fourth disulfide bond (C259–C262) exists within extracellular loop 3 (Figure 1). Two of the disulfide bonds are thought to be unique to hA_{2a}R, while the C77–C166 bond is generally conserved throughout most GPCRs (22). The CXXC motif within the third extracellular loop is also shared by the hA₁ receptor, within the adenosine receptor family (23, 24).

It has been postulated that these four disulfide bonds aid in ligand discrimination and/or ligand accessibility within the binding cavity of hA_{2a}R (4). Here, disulfide bonds in hA_{2a}R-His₁₀ were reduced through incubation with the reducing agent tris-(2-carboxyethyl)phosphine (TCEP) or dithiothreitol (DTT), and reduction was monitored via a reducing gel analysis (Figure 3), previously used to detect disulfide reduction in hA_{2a}R (9). Upon incubation with 0.5 mM TCEP, the band corresponding to the hA_{2a}R-His₁₀ monomer was characterized by altered mobility through the gel (Figure 3A). Upon titration with increasing amounts of TCEP (up to 10 mM), migration of hA_{2a}R-His₁₀ remained unchanged relative to that with the 0.5 mM addition, suggesting that incubation with increasing concentrations of this reducing agent did not bring about further disulfide bond reduction under these conditions.

hA_{2a}R-His₁₀ secondary structure remained highly α -helical in the presence of 1 mM TCEP (Figure 2A), and the fluorescence spectra was relatively unchanged compared to that of native (non-reduced) receptors (data not shown), inferring that reduction of

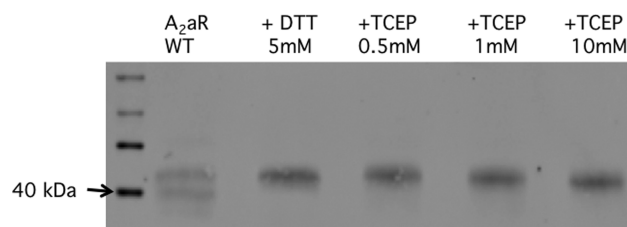


FIGURE 3: Effect of reducing agents on purified, solubilized hA_{2a}R. Samples were incubated with 5 mM DTT or 0.5–10 mM TCEP, separated via 12% SDS–PAGE, and blotted onto nitrocellulose for detection with an anti-His primary antibody. An arrow denotes the molecular mass marker (40 kDa) for MagicMarkWestern protein standard (Life Technologies), close to the mobility of the monomeric band of wild-type hA_{2a}R-His₁₀.

hA_{2a}R's disulfide bonds had no direct effect on the conformation of the unliganded receptor.

Thermal and Chemical Stability of Full-Length hA_{2a}R-His₁₀. One of the barriers to determining the stability of membrane proteins is that the detergent contributes to the stability, resulting in challenges to studying unfolding (25–28). Reversible folding of membrane proteins proves to be among the greatest difficulties associated with their biophysical characterization, and very few α -helical membrane proteins have been folded or unfolded *in vitro* (29, 30).

Thermal denaturation was found to be a useful approach to perturbing hA_{2a}R-His₁₀ conformation. Figure 4 shows representative spectra generated for hA_{2a}R-His₁₀ as measured by CD (Figure 4A) and intrinsic fluorescence spectroscopy (Figure 4B) as temperatures were increased. Unfolding of the hA_{2a}R-His₁₀ secondary structure was characterized by a loss of α -helical structure, as seen through a loss of the characteristic trough at 208 and 222 nm (Figure 4A). Overall, an 80% loss of α -helical content was seen when hA_{2a}R-His₁₀ was heated to 90 °C, and a midpoint of unfolding was fit on the basis of a pseudo-two-state model (Table 1). When the temperature was lowered back to 10 °C, we found that only ~10–20% α -helical content was recovered and these spectra did not overlap with initial measurements at 10 °C

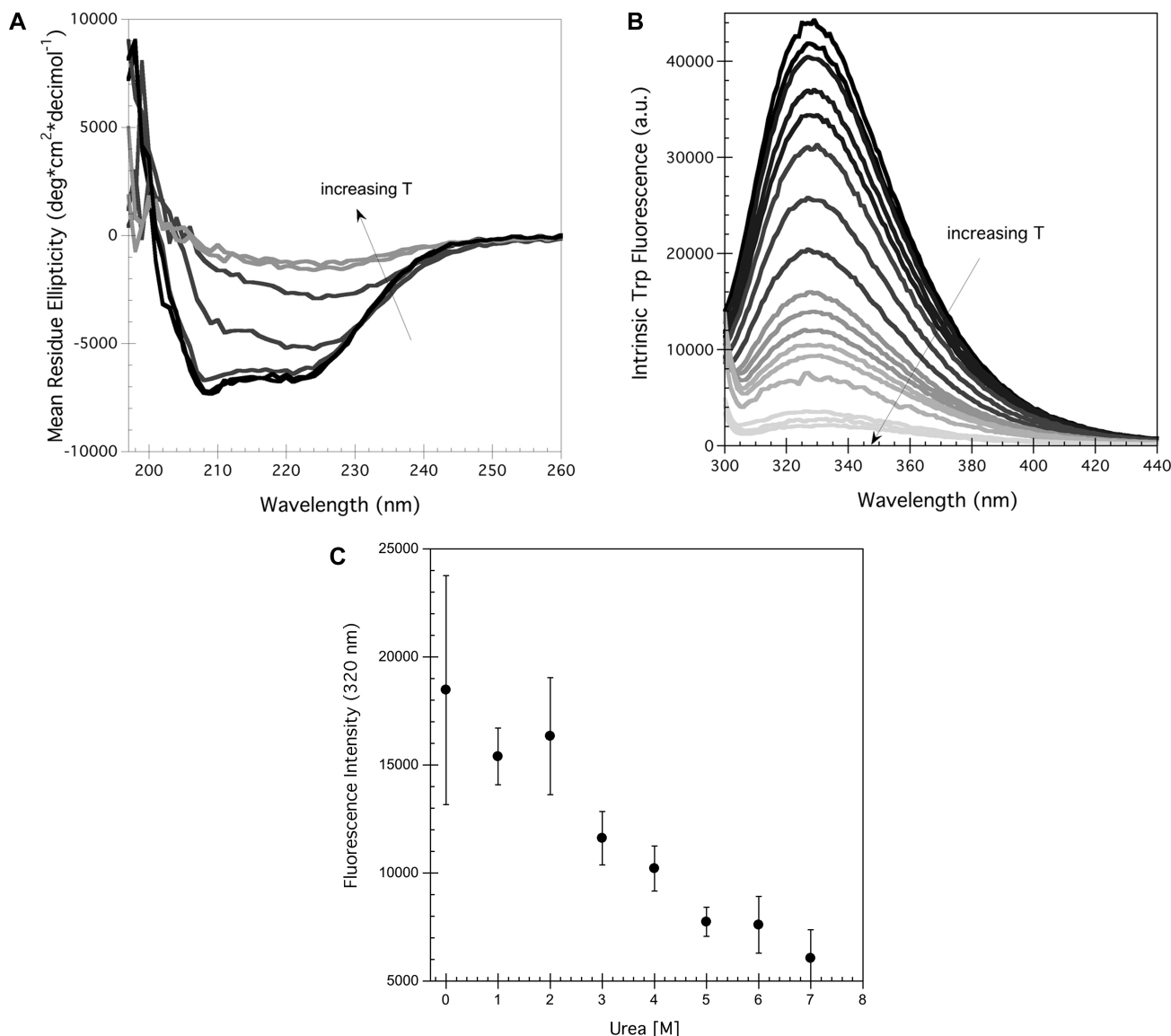


FIGURE 4: (A) Representative thermal unfolding CD spectra obtained for hA₂aR-His₁₀, with temperatures increasing from 5 to 95 °C, in 15 °C increments, where lighter gray lines depict data for higher temperatures. (B) Tertiary structure changes monitored through intrinsic tryptophan fluorescence (excitation wavelength of 290 nm). Spectra represent temperatures from 11 to 79 °C, in 8 °C increments, where lighter gray lines depict data for higher temperatures. (C) Chemical unfolding of hA₂aR-His₁₀ as a function of increasing urea concentration, as determined by intrinsic fluorescence intensity changes at 320 nm. Error bars represent the deviation from the average of two or more biological replicates.

(data not shown), indicating that the thermal unfolding transition was not reversible. It is likely this lack of reversibility results from aggregate formation at > 80 °C, as evidenced by increased absorbance in the visible range (~450–600 nm).

Increasing the temperature from 5 to 95 °C led to a decrease in the tryptophan fluorescence emission intensity but little change in the center of mass (Figure 4B). In the case of hA₂aR, incubation with chemical chaotropes and SDS did not result in well-behaved denaturation, as intrinsic tryptophan fluorescence and CD did not decrease monotonically with an increased concentration of SDS (data not shown) and urea [intrinsic tryptophan fluorescence (Figure 4C)], consistent with the temperature denaturation, but unlike that of many small soluble proteins (31, 32). When the full-length, purified hA₂aR-His₁₀ was incubated with 0–2 M urea, the intrinsic tryptophan fluorescence intensity at 320 nm remained approximately the same and then decreased rapidly above 2 M urea (Figure 4C).

Thermal Unfolding of hA₂aR-His₁₀ upon Ligand Addition. To determine the effect of ligands on hA₂aR-His₁₀ stability,

molar ellipticities at 222 nm as a function of temperature were determined (Figure 5A). Although the thermal denaturation was only partly reversible, a single transition between two states was observed in the CD data (Figure 5A). For hA₂aR-His₁₀, this unfolding transition occurred at 58.9 ± 0.4 °C (Table 1). In the presence of the agonist CHA and the antagonist theophylline (Theo), changes to the thermal stability relative to hA₂aR-His₁₀ alone were observed (Figure 5A). In the agonist-bound state, the hA₂aR-His₁₀ secondary structure was slightly more resistant to thermal denaturation than the unliganded protein or protein bound to the antagonist, as a slight increase in the overall midpoint of unfolding was seen only in the presence of CHA (61.1 ± 0.6 °C) (Table 1).

In these studies, we used an additional fluorescence-based reporter system as a complementary method to elucidate tertiary structure changes and folding transitions for hA₂aR-His₁₀. The thiol-reactive probe 7-(diethylamino)-3-(4'-maleimidylphenyl)-4-methylcoumarin (CPM), which reacts with solvent-exposed cysteines, was utilized, as it has been useful for studying unfolding

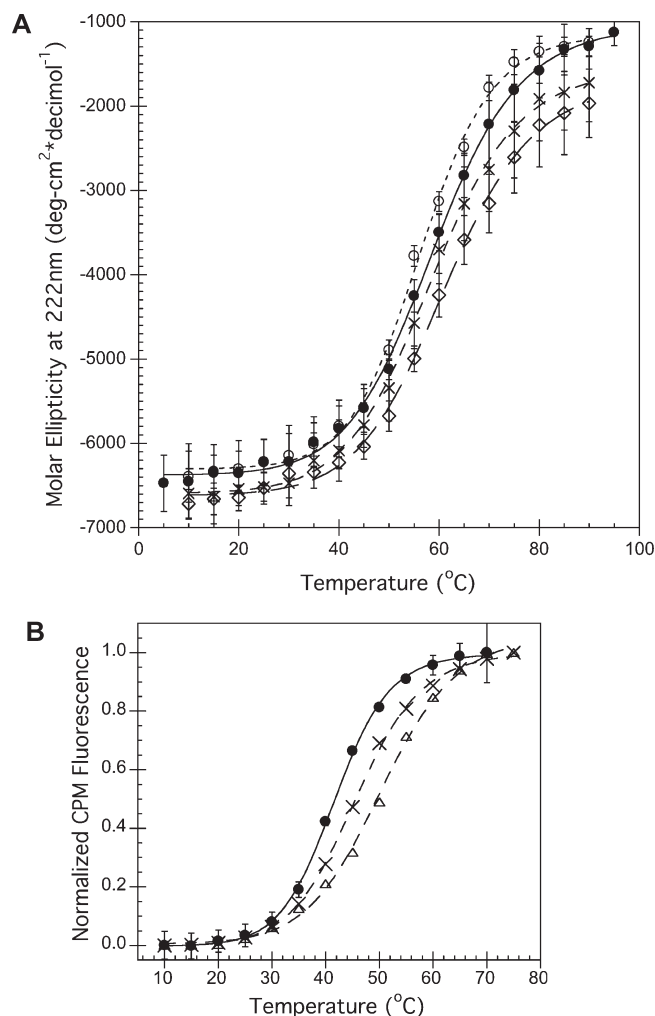


FIGURE 5: Thermal unfolding of hA₂aR-His₁₀ monitored via CD at 222 nm (A) or via the fluorescence intensity (at 463 nm) of a thiol-reactive fluorescent probe, CPM (B), for unliganded receptors (●), receptors with 100 μM CHA agonist (◇) or with 1000 μM theophylline antagonist (×), and receptors reduced with 1 mM TCEP (○). Lines represent fits to a single-transition folding model for experimental data (points). Error bars represent the standard deviation from the average of three or more trials.

of membrane proteins (4, 21). Upon addition of CPM to purified hA₂aR-His₁₀, the observed fluorescence emission at 463 nm increased by a factor of nearly 10 (data not shown). Note that for hA₂aR, the reporter groups for CPM binding are six trans-membrane cysteine residues and one cysteine on the C-terminal end of the protein (Figure 1).

Addition of CHA (agonist) or theophylline (antagonist) to hA₂aR-His₁₀ yielded a distinct shift in the unfolding behavior from that of the unliganded hA₂aR-His₁₀ when fluorescence (due to CPM binding) was examined as a function of temperature (Figure 5B). When fit to an unfolding model that describes a single transition between two states, effective $T_{1/2}$ values were 41.7 ± 0.2 °C for unliganded hA₂aR-His₁₀, which increased to 46.3 ± 0.5 °C for hA₂aR-His₁₀ bound to CHA and 45.6 ± 0.2 °C for hA₂aR-His₁₀ bound to theophylline (Table 1 and Figure 5B).

Thermal Unfolding of hA₂aR-His₁₀ upon TCEP Addition. Because of the increased protein stability usually imparted to proteins via disulfide linkages (33–35), we explored whether these bonds also play a role in the stabilization of hA₂aR. The thermal denaturation of disulfide-reduced hA₂aR-His₁₀ monitored via CD led to a thermal midpoint of unfolding at $55.9 \pm$

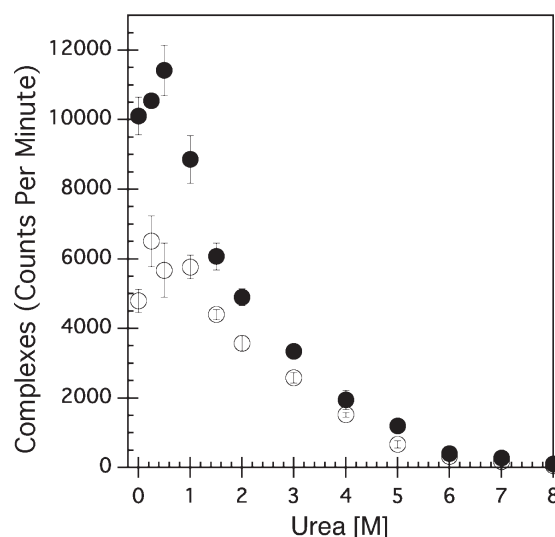


FIGURE 6: Denaturation of hA₂aR-His₁₀ via urea addition leads to a loss of receptor ligand binding activity (decrease in the level of receptor–ligand complexes) as measured through radioligand binding with [³H]CGS-21,680 in the presence (○) or absence (●) of the reducing agent TCEP. Error bars depict the standard deviation from the average of three replicate samples at each urea concentration.

0.4 °C, ~3 °C lower than that of untreated hA₂aR-His₁₀ (Figure 5A and Table 1). However, CPM fluorescence could not be determined, as TCEP addition (even in modest amounts) to CPM resulted in a pronounced increase in fluorescence intensity, which masked any folding transitions obtained.

To determine whether the disulfide bond network in the extracellular loops of hA₂aR impacted ligand binding as a metric for tertiary structure stability, surfactant-reconstituted receptors in the presence or absence of TCEP were incubated with urea to perturb protein structure. Receptor activity via radioligand binding was used as a sensitive metric to assess the folded state for disulfide bond-reduced hA₂aR-His₁₀. In this set of experiments, hA₂aR-His₁₀ or reduced hA₂aR-His₁₀ protein was bound to the same concentration of [³H]CGS-21,680 (a high-affinity A₂aR agonist) over a range of urea concentrations (0–8 M). As seen in Figure 6, in the absence of urea, reduced receptors exhibited diminished activity compared to that of native hA₂aR-His₁₀, by approximately 40%. At low urea concentrations (<1 M), the bound ligand obtained for hA₂aR-His₁₀ and reduced hA₂aR-His₁₀ was relatively unaffected compared to 0 M urea, as solubilized receptors largely maintained their maximal ligand binding activity (Figure 6). Upon incubation with increasing amounts of urea, a sharp decrease in obtained radioactivity was observed, likely due to a decrease in receptor activity caused by urea-associated unfolding. Both native and reduced hA₂aR-His₁₀ proteins lost approximately half of their binding affinity at ~2 M urea. When 6 M urea was reached, most ligand binding activity for hA₂aR-His₁₀ was eliminated, in the presence or absence of TCEP.

DISCUSSION

In this study, biophysical characterization of the full-length human adenosine A₂a receptor (hA₂aR) was performed to improve our understanding of receptor conformational changes and stability in the presence of extracellular ligands. We also investigated hA₂aR conformational stability in the presence of a reducing agent, because extensive disulfide bonding within the

receptor's extracellular loop regions was found within the crystal structure (4).

Slight Conformational Changes Accompany Ligand Binding. Biophysical methods were employed to examine changes in protein conformation upon binding of agonist and antagonist molecules to hA_{2a}R-His₁₀. From CD measurements, we were not able to detect appreciable changes in the receptor's α -helical secondary structure when bound to ligands (Figure 2A). One can infer from these data that receptor α -helical content does not change significantly during ligand binding. Therefore, it is more likely that transmembrane domain α -helices within hA_{2a}R-His₁₀ shift upon extracellular ligand binding rather than incur any direct change to their α -helical conformation.

Although the fluorescence emission maximum remained unchanged for several conditions tested, a slight, reproducible shift was seen for hA_{2a}R-His₁₀ only in the presence of agonist (Figure 2B). Similar blue-shift behavior in the intrinsic fluorescence spectrum of agonist-bound GPCRs has also been reported for the BLT₁ receptor upon binding LTB₄ (36). Because there was a relatively small change in the emission maximum upon ligand binding (Figure 2B), we can infer that the average environment of the tryptophans in hA_{2a}R-His₁₀ does not undergo a major change.

A significant reduction in the magnitude of the fluorescence signal accompanied both agonist and antagonist binding relative to hA_{2a}R-His₁₀ in the absence of ligands, indicating that both ligands bury Trp residues of the receptor (Figure 2B). A larger decrease in fluorescence intensity in the presence of CHA compared to that with theophylline indicates that CHA binding affects the solvation state of more Trp residues of the receptor than theophylline does upon its binding.

Solvent-exposed regions of GPCRs have been hypothesized to play a role in accommodating ligand binding in both rhodopsin and β_2 AR (37), which likely also explains the Trp fluorescence decreases observed here, because many Trp residues within hA_{2a}R are located at the interface of transmembrane helices and soluble loops, with Trp 246 at a critical site in the ligand binding pocket (7).

hA_{2a}R Thermal and Chemical Denaturation. We have used thermal denaturation to characterize the unfolding pathway for solubilized hA_{2a}R-His₁₀ under a variety of conditions. Thermal unfolding of receptor secondary structure was described well as a single transition between two folded states (Figure 5A), as was thermal unfolding of tertiary structure when CPM was used to monitor cysteine accessibility (Figure 5B). Thermal unfolding monitored by CD spectroscopy was used to evaluate protein stability in the presence of ligand. As with many soluble (38) and membrane-bound proteins (39), the equilibrium thermodynamic analysis of the unfolding of hA_{2a}R-His₁₀ was hampered by irreversibility, because of aggregates formed to some degree with an increased temperature. Therefore, it is important to clarify that folding transitions reported in this study are effective midpoints of unfolding, rather than equilibrium unfolding parameters.

The ellipticity was only slightly affected by temperature changes between 20 and 50 °C, indicating that secondary structure is stable within this temperature range (Figure 4A). At higher temperatures, the spectra change gradually with an increase in temperature (Figure 3A), as the minimum at 222 nm broadens and loses its intensity, suggesting unfolding of the protein. Our data show that large heat-induced increases in the scattering (corresponding to greater than 300 V) that would be indicative of

aggregation of partially unfolded protein take place only above ~80–85 °C, which is much higher than calculated $T_{1/2}$ values (Table 1).

It is important to note that a simple two-state folding–unfolding transition is characterized by two states only, the native state and the denatured state, with a single cooperative transition. However, here the midpoint of unfolding calculated via CD and CPM fluorescence for hA_{2a}R-His₁₀ did not occur at the same temperature: the secondary structure transition observed by CD occurred at 58.9 °C, while the tertiary structure transition monitored by CPM binding took place at 41.7 °C for unliganded receptors. This unfolding behavior is consistent with the unfolding model proposed by Popot and Engelman for α -helical membrane proteins, whereby α -helices act as stable, independent folding domains, and their interaction defines the tertiary structure that undergoes a separate folding transition (40). Such behavior has been observed previously for the well-studied GPCR rhodopsin, whereby pH-induced denaturation led to a loss of tertiary contacts between the receptor and retinal, yet secondary structure was largely intact as monitored via FTIR (41). Simulation of the thermal unfolding of rhodopsin has suggested that denaturation begins with a loss of hydrogen bonds and disulfide bridges within extracellular loops, which is directly coupled to the orientation of transmembrane helices, although they do not fully unfold (42). An alternate explanation is that a change in permeability or structure of the micelles at increasing temperatures allows the CPM probe to enter the transmembrane domains before denaturation, or the probe itself may facilitate protein denaturation. Although dodecyl maltoside has a critical micelle concentration (CMC) of ~0.2 mM at 25 °C (43, 44), we are working at ~16 times the CMC of pure surfactant at 25 °C, and the temperature dependence of micelle formation is expected to be weak (~0.25 mM at 50 °C) (43). However, we cannot rule out some changes in micelle structure or permeability with an increase in temperature. A further consideration is that due to high hydrophobicity, α -helices in membrane proteins may not denature to the same extent usually seen in soluble proteins (29).

In comparing unfolding of hA_{2a}R-His₁₀ using both conformational probes (tryptophan and CPM fluorescence), we have found that receptors bound to CHA and theophylline demonstrated enhanced stability compared to that of the unliganded receptor. Here we observe that wild-type hA_{2a}R-His₁₀ was ~3–4 °C less stable than the engineered protein hA_{2a}R-T4L- Δ C, which includes a C-terminal truncation and replacement of intracellular loop 3 with T4 lysozyme (4). Interestingly, Stevens and colleagues reported increased thermal stability in the presence of certain antagonists (4), consistent with our observations for theophylline binding to the full-length native receptor; however, they did not observe any changes in stability upon agonist binding. In contrast, we can observe a significant increase in GPCR stability in the presence of the agonist CHA for the full-length receptor.

The Extracellular Disulfide Network Is Critical to Ligand Binding. No changes were immediately observed within either the hA_{2a}R-His₁₀ secondary structure (Figure 2A) or tertiary structure (as measured through intrinsic Trp fluorescence) when disulfide bonds were reduced with TCEP. However, for reduced hA_{2a}R-His₁₀, the $T_{1/2}$ calculated from thermal denaturation as observed by CD was 55.9 °C, which is approximately 3 °C less stable than unliganded hA_{2a}R-His₁₀ (Figure 5A and Table 1).

When hA_{2a}R-His₁₀ was incubated with the reducing agent TCEP, ~40% of the ligand binding activity was lost (Figure 6).

Although at least partial reduction of disulfide bonds in hA₂aR-His₁₀ was achieved in this study (Figure 3), it is important to note that the entire network may not have been fully disrupted. Other studies have shown that reducing agents, presumably acting to reduce disulfide bonds within extracellular loops, can diminish the activity of h β ₂AR (45, 46), the μ -opioid receptor (47), and a human thromboxane receptor (48). Loss of ligand binding activity as a function of urea concentration follows a similar trend for hA₂aR-His₁₀ and reduced hA₂aR-His₁₀, which implies that the tertiary structure unfolding pathways are likely analogous (Figure 6). Therefore, these experiments support the conclusion that while hA₂aR activity is sensitive to disulfide bonding within extracellular loops, likely due to ligand accessibility within the agonist-binding site, disulfide bonding does not necessarily impart significant tertiary structural stability to the protein.

CONCLUSION

Biophysical studies conducted with full-length, solubilized hA₂aR-His₁₀ have shown important receptor behavior under a variety of conditions and have allowed for the identification of critical factors that influence stability. We have seen that while slight changes for hA₂aR-His₁₀ tertiary structure are evident, either agonist or antagonist binding significantly increased the overall stability as observed in both receptor secondary and tertiary structure folding transitions. In addition to the insight drawn from these studies for hA₂aR-His₁₀, the approach developed here may be further applied to other GPCRs to characterize whether these small changes in conformation upon ligand binding and stabilizing effects are commonly shared among other adenosine receptors, or even more broadly shared between members of the GPCR superfamily.

ACKNOWLEDGMENT

We thank Dr. K. Dane Wittrup (Massachusetts Institute of Technology, Cambridge, MA) for the pITy plasmid and Dr. Marlene Jacobson (Merck) for the human adenosine A₂a receptor gene.

REFERENCES

- Kobilka, B., and Schertler, G. F. X. (2008) New G-protein-coupled receptor crystal structures: Insights and limitations. *Trends Pharmacol. Sci.* 29, 79–83.
- Chiu, M. L., Tsang, C., Grihalde, N., and MacWilliams, M. P. (2008) Over-expression, solubilization, and purification of G protein-coupled receptors for structural biology. *Comb. Chem. High Throughput Screening* 11, 439–462.
- Cherezov, V., Rosenbaum, D. M., Hanson, M. A., Rasmussen, S. G. F., Thian, F. S., Kobilka, T. S., Choi, H. J., Kuhn, P., Weis, W. I., Kobilka, B. K., and Stevens, R. C. (2007) High-resolution crystal structure of an engineered human β_2 -adrenergic G protein-coupled receptor. *Science* 318, 1258–1265.
- Jaakola, V. P., Griffith, M. T., Hanson, M. A., Cherezov, V., Chien, E. Y. T., Lane, J. R., Ijzerman, A. P., and Stevens, R. C. (2008) The 2.6 Ångstrom Crystal Structure of a Human A(2A) Adenosine Receptor Bound to an Antagonist. *Science* 322, 1211–1217.
- Palczewski, K., Kumasaka, T., Hori, T., Behnke, C. A., Motoshima, H., Fox, B. A., Le Trong, I., Teller, D. C., Okada, T., Stenkamp, R. E., Yamamoto, M., and Miyano, M. (2000) Crystal structure of rhodopsin: A G protein-coupled receptor. *Science* 289, 739–745.
- Warne, T., Serrano-Vega, M. J., Baker, J. G., Moukhametzianov, R., Edwards, P. C., Henderson, R., Leslie, A. G. W., Tate, C. G., and Schertler, G. F. X. (2008) Structure of a β_1 -adrenergic G-protein-coupled receptor. *Nature* 454, 486–491.
- Jaakola, V. P., Lane, J. R., Lin, J. Y., Katritch, V., Ijzerman, A. P., and Stevens, R. C. (2010) Ligand Binding and Subtype Selectivity of the Human A(2A) Adenosine Receptor. Identification and Characterization of Essential Amino Acid Residues. *J. Biol. Chem.* 285, 13032–13044.
- Katritch, V., Jaakola, V. P., Lane, J. R., Lin, J., Ijzerman, A. P., Yeager, M., Kufareva, I., Stevens, R. C., and Abagyan, R. (2010) Structure-Based Discovery of Novel Chemotypes for Adenosine A(2A) Receptor Antagonists. *J. Med. Chem.* 53, 1799–1809.
- Butz, J. A., Niebauer, R. T., and Robinson, A. S. (2003) Co-expression of molecular chaperones does not improve the heterologous expression of mammalian G-protein coupled receptor expression in yeast. *Bio-technol. Bioeng.* 84, 292–304.
- Niebauer, R. T., and Robinson, A. S. (2006) Exceptional total and functional yields of the human adenosine (A₂a) receptor expressed in the yeast *Saccharomyces cerevisiae*. *Protein Expression Purif.* 46, 204–211.
- Niebauer, R. T., Wedekind, A., and Robinson, A. S. (2004) Decreases in yeast expression yields of the human adenosine A₂a receptor are a result of translational or post-translational events. *Protein Expression Purif.* 37, 134–143.
- O'Malley, M. A., Lazarova, T., Britton, Z. T., and Robinson, A. S. (2007) High-level expression in *Saccharomyces cerevisiae* enables isolation and spectroscopic characterization of functional human adenosine A(2)a receptor. *J. Struct. Biol.* 159, 166–178.
- O'Malley, M. A., Mancini, J. D., Young, C. L., McCusker, E. C., Raden, D., and Robinson, A. S. (2009) Progress toward heterologous expression of active G-protein-coupled receptors in *Saccharomyces cerevisiae*: Linking cellular stress response with translocation and trafficking. *Protein Sci.* 18, 2356–2370.
- Vangalen, P. J. M., Stiles, G. L., Michaels, G., and Jacobson, K. A. (1992) Adenosine-a(1) and Adenosine-a(2) Receptors: Structure-Function Relationships. *Med. Res. Rev.* 12, 423–471.
- Piersen, C. E., True, C. D., and Wells, J. N. (1994) A carboxyl-terminally truncated mutant and nonglycosylated A₂a adenosine receptors retain ligand binding. *Mol. Pharmacol.* 45, 861–870.
- Price, L. A., Strnad, J., Pausch, M. H., and Hadcock, J. R. (1996) Pharmacological characterization of the rat A₂a adenosine receptor functionally coupled to the yeast pheromone response pathway. *Mol. Pharmacol.* 50, 829–837.
- Muller, C. E. (2000) A(2A) adenosine receptor antagonists: Future drugs for Parkinson's disease? *Drugs Future* 25, 1043–1052.
- Jarvis, M. F., Schulz, R., Hutchison, A. J., Do, U. H., Sills, M. A., and Williams, M. (1989) [H-3] Cgs-21680, a Selective A₂ Adenosine Receptor Agonist Directly Labels A₂-Receptors in Rat-Brain. *J. Pharmacol. Exp. Ther.* 251, 888–893.
- Hirs, C. H. W., and Timasheff, S. N. (1986) Methods in Enzymology, Vol. 131, Harcourt Brace Jovanovich, Orlando, FL.
- Stoscheck, C. M. (1990) Quantitation of Protein. *Methods Enzymol.* 182, 50–68.
- Alexandrov, A. I., Mileni, M., Chien, E. Y. T., Hanson, M. A., and Stevens, R. C. (2008) Microscale fluorescent thermal stability assay for membrane proteins. *Structure* 16, 351–359.
- Lagerstrom, M. C., and Schioth, H. B. (2008) Structural diversity of G protein-coupled receptors and significance for drug discovery. *Nat. Rev. Drug Discovery* 7, 339–357.
- Fredholm, B. B., Abbracchio, M. P., Burnstock, G., Daly, J. W., Harden, T. K., Jacobson, K. A., Leff, P., and Williams, M. (1994) Nomenclature and Classification of Purinoceptors. *Pharmacol. Rev.* 46, 143–156.
- Cristalli, G., Lambertucci, C., Marucci, G., Volpini, R., and Dal Ben, D. (2008) A(2A) adenosine receptor and its modulators: Overview on a druggable GPCR and on structure-activity relationship analysis and binding requirements of agonists and antagonists. *Curr. Pharm. Des.* 14, 1525–1552.
- Hong, H., Joh, N. H., Bowie, J. U., and Tamm, L. K. (2009) Methods for Measuring the Thermodynamic Stability of Membrane Proteins. In *Methods in Enzymology: Biothermodynamics*, Vol. 455, Part A, pp 213–236, Elsevier Academic Press Inc., San Diego.
- Rosenbusch, J. P. (2001) Stability of membrane proteins: Relevance for the selection of appropriate methods for high-resolution structure determinations. *J. Struct. Biol.* 136, 144–157.
- Stowell, M. H. B., and Rees, D. C. (1995) Structure and Stability of Membrane-Proteins. In *Advances in Protein Chemistry*, Vol. 46, pp 279–311, Academic Press Inc., San Diego.
- Haltia, T., and Freire, E. (1995) Forces and Factors That Contribute to the Structural Stability of Membrane-Proteins. *Biochim. Biophys. Acta* 1228, 1–27.
- Booth, P. J., and Curnow, P. (2006) Membrane proteins shape up: Understanding in vitro folding. *Curr. Opin. Struct. Biol.* 16, 480–488.
- Bowie, J. U. (2005) Solving the membrane protein folding problem. *Nature* 438, 581–589.

31. Dill, K. A., Ozkan, S. B., Shell, M. S., and Weikl, T. R. (2008) The protein folding problem. *Annu. Rev. Biophys.* 37, 289–316.
32. Gianni, S., Ivarsson, Y., Bah, A., Bush-Pelc, L. A., and Di Cera, E. (2007) Mechanism of Na⁺ binding to thrombin resolved by ultra-rapid kinetics. *Biophys. Chem.* 131, 111–114.
33. Clarke, J., and Fersht, A. R. (1993) Engineered Disulfide Bonds as Probes of the Folding Pathway of Barnase: Increasing the Stability of Proteins against the Rate of Denaturation. *Biochemistry* 32, 4322–4329.
34. Creighton, T. E., and Goldenberg, D. P. (1984) Kinetic Role of a Metastable Native-Like 2-Disulfide Species in the Folding Transition of Bovine Pancreatic Trypsin-Inhibitor. *J. Mol. Biol.* 179, 497–526.
35. Wedemeyer, W. J., Welker, E., Narayan, M., and Scheraga, H. A. (2000) Disulfide bonds and protein folding. *Biochemistry* 39, 4207–4216.
36. Baneres, J. L., Martin, A., Hullot, P., Girard, J. P., Rossi, J. C., and Parello, J. (2003) Structure-based analysis of GPCR function: Conformational adaptation of both agonist and receptor upon leukotriene B-4 binding to recombinant BLT1. *J. Mol. Biol.* 329, 801–814.
37. Blumer, K. J., and Thorner, J. (2007) An adrenaline (and gold?) rush for the GPCR community. *ACS Chem. Biol.* 2, 783–786.
38. Duy, C., and Fitter, J. (2006) How aggregation and conformational scrambling of unfolded states govern fluorescence emission spectra. *Biophys. J.* 90, 3704–3711.
39. Lau, F. W., and Bowie, J. U. (1997) A method for assessing the stability of a membrane protein. *Biochemistry* 36, 5884–5892.
40. Popot, J. L., and Engelman, D. M. (1990) Membrane-Protein Folding and Oligomerization: The 2-Stage Model. *Biochemistry* 29, 4031–4037.
41. Vogel, R., and Siebert, F. (2002) Conformation and stability of α -helical membrane proteins. 2. Influence of pH and salts on stability and unfolding of rhodopsin. *Biochemistry* 41, 3536–3545.
42. Rader, A. J., Anderson, G., Isin, B., Khorana, H. G., Bahar, I., and Klein-Seetharaman, J. (2004) Identification of core amino acids stabilizing rhodopsin. *Proc. Natl. Acad. Sci. U.S.A.* 101, 7246–7251.
43. Aoudia, M., and Zana, R. (1998) Aggregation Behavior of Sugar Surfactants in Aqueous Solutions: Effects of Temperature and the Addition of Nonionic Polymers. *J. Colloid Interface Sci.* 206, 158–167.
44. Drummond, C. J., Warr, G. G., Grieser, F., Ninham, B. W., and Evans, D. F. (1985) Surface Properties and Micellar Interfacial Microenvironment of N-Dodecyl- β -D-Maltoside. *J. Phys. Chem.* 89, 2103–2109.
45. Pedersen, S. E., and Ross, E. M. (1985) Functional Activation of β -Adrenergic Receptors by Thiols in the Presence or Absence of Agonists. *J. Biol. Chem.* 260, 4150–4157.
46. Prior, T. I., Patel, V., and Drummond, G. I. (1985) Inactivation of the β -Adrenergic-Receptor in Cardiac Muscle by Dithiols. *Can. J. Physiol. Pharmacol.* 63, 932–936.
47. Zhang, P. S., Johnson, P. S., Zollner, C., Wang, W. F., Wang, Z. J., Montes, A. E., Seidleck, B. K., Blaschak, C. J., and Surratt, C. K. (1999) Mutation of human mu opioid receptor extracellular “disulfide cysteine” residues alters ligand binding but does not prevent receptor targeting to the cell plasma membrane. *Mol. Brain Res.* 72, 195–204.
48. Dangelo, D. D., Eubank, J. J., Davis, M. G., and Dorn, G. W. (1996) Mutagenic analysis of platelet thromboxane receptor cysteines: Roles in ligand binding and receptor-effector coupling. *J. Biol. Chem.* 271, 6233–6240.